

Detecting Satellite Maneuver Intent Using Game Theory

Guanchu He

Department of Computer Science, University of Colorado Colorado Springs (UCCS), United States

Philip N. Brown

Department of Computer Science, University of Colorado Colorado Springs (UCCS), United States

Kaylee Barcroft

Astra Ultra, United States

Jeffrey Smith

Astra Ultra, United States

Matthew Bonn

Astra Ultra, United States

Josué Cardoso dos Santos

Department of Mechanical and Aerospace Engineering, University of Colorado Colorado Springs (UCCS), United States

Jackson Thorne

Department of Mechanical and Aerospace Engineering, University of Colorado Colorado Springs (UCCS), United States

ABSTRACT

Space Domain Awareness (SDA) requires real-time assessment of satellite maneuvers to distinguish benign trajectory adjustments from potentially hostile actions. Currently, intent classification relies on manual analysis, which is slow, labor-intensive, and susceptible to ambiguity. Furthermore, if an intelligent adversary knows that it is being monitored, it can potentially use complicated sequences of maneuvers to attempt to mask hostile maneuvers as benign. Alternatively, an adversary could deceptively attempt to mask benign maneuvers as hostile in an attempt to desensitize a defender's intent classifier. Either of these approaches may substantially add to the defender's intent classification challenge. To address this challenge, we propose a game-theoretic framework that models maneuver interactions between a defending satellite ("Blue") and a potentially adversarial satellite ("Red") which may intend to execute a kinetic attack against Blue. This framework will enable automated inference of maneuver intent by formulating the interaction as a game with asymmetric information.

In this model, Red transitions from a benign state to a threatening state at an unknown time, while Blue must infer this transition by observing Red's kinematics. We propose several baseline parameterized alert strategies for Blue which react to Red's motion history and predicted future trajectories, including a range of approaches from simple threshold-based triggers to advanced receding-horizon methods that estimate Red's minimum time-to-collision. In response, Red can probe these alert strategies and attempt to induce false positive alerts early in the interaction or execute a stealthy attack late in the interaction. We adopt a leader-follower ("Stackelberg") style interaction, in which Blue pre-commits

*This material is based upon work supported by the Air Force Office of Scientific Research under award numbers FA9550-25-P-B001 and FA9550-23-1-0171. Any opinions, findings and conclusions or recommendations expressed in this material are those of the author(s) and do not necessarily reflect the views of the United States Air Force.

to an alert strategy and then Red responds to attempt to maximize the probability of a successful kinetic attack at the end of the interaction. We constrain the actions of both satellites (with hard delta- v and rate limits on Red’s maneuvers and limits on the total time over which Blue can alert). We believe that this game-theoretic modeling approach offers a principled approach to maneuver intent classification.

To begin to instantiate the model in a way that ingests real-world data, we propose a novel intent classification method which ingests TLE updates for a Red/Blue satellite pair and uses solutions to Lambert’s problem to identify future opportunities for the Red satellite to execute a kinetic attack on the Blue satellite. We then validate our approach by applying it to several historical examples of known RPO events. For instance, the 2009 HTV-1 resupply mission to the International Space Station has a list of known maneuvers which we can use as a ground truth to assess the effectiveness of our intent classifier. We show that our techniques correctly classify all of the known maneuvers made by HTV-1 during its approach to the ISS.

By leveraging this framework, we demonstrate how real-time data assimilation techniques—coupled with strategic decision models—can enhance SDA automation. Our results suggest that incorporating adversarial reasoning into SDA algorithms can significantly improve automated threat assessment, reducing reliance on manual intervention while maintaining operational accuracy. This research has direct implications for space security, as it provides a principled method for autonomous human-on-the-loop decision support in SDA. Future work will focus on integrating this framework with advanced strategic modeling and refining alert thresholds through reinforcement learning techniques. In addition, the modularity of our approach will enable us to study a wide variety of attack models.

1. INTRODUCTION

Satellites play a critical role in a wide range of military and civilian applications, making them potential targets of various threats. Such satellite threats or attacks can be defined as deliberate or unintentional actions that compromise a satellite’s functionality or integrity. In either case, these attacks can lead to irreversible damage and catastrophic failures of crucial systems. There are four major types of satellite attacks: kinetic physical attacks (e.g., physical impact or explosion), non-kinetic physical attacks (e.g., laser or high-energy weapons), electronic attacks (e.g., blocking satellite signals), and cyber attacks (e.g., malware injection) [9, 37, 51, 45]. Among these forms of attack, co-orbital stalking maneuvers that bring a satellite close to each other can serve as a precursor to any of the disruptive attack types. Accordingly, the timely detection of such co-orbital maneuvers at the earliest possible stage is of critical importance for preventing potential attacks.

Space Domain Awareness (SDA) focuses on gathering data and understanding potential threats and intentions that could affect space assets. This includes ensuring safe satellite operations, preventing collisions, and maintaining national security and strategic advantage in space. A maneuver can suddenly escalate into a hostile attack if triggered by external instructions. Consequently, such maneuvers may initially appear benign, seem unintentional, or not resemble maneuvers at all until the moment of attack. This highlights the importance of developing methods to detect hostile maneuvers early, before they become apparent and unstoppable. As a result, within the broader SDA framework, co-orbital maneuver detection is a critical task [25, 44, 17]. Building on this context, this paper narrows its focus to real-time assessment of satellite maneuvers in order to discriminate between benign orbital adjustments and hostile maneuvers.

Current maneuver detection methods rely heavily on manual analysis and human filtering [26, 16], which can lead to missed detections, particularly for slow or subtle maneuvers. These manual approaches are also susceptible to deliberate deception and less effective against intelligent adversaries. Consequently, the likelihood of failing to detect hostile maneuvers increases. To our knowledge, current research addresses machine learning based anomaly detection trained on historical orbital maneuver data [10], catalog filtering [4], two-line element set (TLE) consistency check [30], and pattern-of-life (POL) analysis of satellites [24, 38], among others. However, only limited research focuses on detecting maneuvers in fast-response settings using sparse orbital propagation information. Given these limitations, research on automated approaches to inferring and categorizing potentially hostile intent in adversarial orbital maneuvers is essential.

Our paper introduces a first principles-based game-theoretic model for automatic maneuver detection and intent classification. The key challenge we address is how to automatically detect potential threats and assign intent scores for adversarial orbital maneuvers at an early stage, using only minimal and the most recent TLE data.

Specifically, our paper proposes an alerting strategy which is designed to monitor the earliest possible collision risk between a defending satellite (Blue) and a potential attacker (Red), under the assumption that Red may execute an optimal impulsive maneuver at any point in the future. Details of Blue’s strategy can be found at Table 1. In our proposal, the Lambert transfer is utilized to compute transfer trajectories and compute the TOF for Red to intercept Blue, assuming a fixed ΔV budget for Red. Specifically, our approach then calculates the minimal time of flight (TOF) across all feasible hypothetical maneuvers up to a magnitude of ΔV at each possible epoch derived from the TLE data.

We validate our framework using real-world orbital rendezvous datasets, including maneuvers involving the International Space Station (ISS), USA-245, and Russia’s KOSMOS 2542/2543, as well as China’s Shijian (SJ)-21 and SJ-25 satellites. Results show that the intent-score alert, analyzed with documented maneuver events, can detect subtle changes even when satellites are nearby and the maneuvers are not visually obvious.

2. RELATED WORK

The model proposed in this paper is based on the fundamentals of game theory and Lambert’s problem. Specifically, for the game theory portion, our model combines the pursuit-evasion framework with the Stackelberg model, both of which are important subcategories of differential games.

2.1 Game Theory

Game theory, the study of interactive strategic decision-making, has been widely applied to analyze a variety of settings including transportation networks [19], multiagent resource allocation [39, 42], cybersecurity [14], and defense interactions [43]. In the context of maneuver intent detection, game theory is relevant because of the strategic interaction between the potentially-adversarial satellite operators. In a *Stackelberg* game setting, one player acts as the leader, committing to a strategy first, while the other player, the follower, responds optimally [49]. In our problem, the Blue player is modeled as the leader, following predefined alert strategies; then, the Red player is modeled as the follower, trying to optimally target the Blue satellite without triggering early warnings. Once these strategies are determined within the game-theoretic framework, they must be translated into executable orbital maneuvers in the space domain.

The pursuit–evasion game describes a scenario in which the pursuer attempts to capture the evader, while the evader seeks to escape capture [50]. However, in our setting, we modify the pursuit–evasion game so that Red must switch its role to pursuer after receiving an instruction, whereas Blue cannot escape but can only raise an alert (see Section 3). Satellite applications increasingly use pursuit–evasion game formulations for tracking, interception, and defensive maneuver analysis.

2.2 Lambert’s Problem

Lambert’s problem is a classical problem in astrodynamics. It determines the trajectory that connects two specified position vectors, \mathbf{r}_1 and \mathbf{r}_2 , within a given TOF, Δt . The Lambert problem plays a central role in several key applications, including initial orbit determination (IOD), transfer orbits, and intercept or targeting problems. In particular, the targeting problem involves determining a transfer trajectory that allows a satellite to move from one orbit to a specified point on another, a formulation widely applied in scenarios such as spacecraft rendezvous and docking with a space station [5, 48]. In our work, we apply the Lambert problem to the transfer or targeting scenario in which Red transfer from its own orbit to Blue’s orbit to intercept Blue. We search across the required TOFs and find the minimum value of TOFs, subject to an upper limit on ΔV .

2.3 Maneuver Intent Detection

Because much of the research on space maneuver intent detection in defense and intelligence is classified and restricted, advanced studies in this area are not publicly available, making academic referencing difficult. The limited existing improvement primarily focuses on enhancing sensor capabilities [2], estimation and filtering approaches [27], categorizing satellite maneuvers based on a substantial amount of historical trajectories [31], and so on.

Among all the publicly revealed methods, Lambert transfers are commonly used in maneuver detections. Beyond Lambert-based approaches, many studies focus on using machine learning methods to categorize types of intent-related motion, among which supervised learning with human-generated labels or an extensive history of trajectories are heavily used. For example, to classify satellite maneuver intentions, the authors of [31] utilized a Convolutional Neural Network (CNN)-based framework that transforms relative orbital trajectories into eleven malicious intent categories.

Similarly, other researches [26, 16, 38, 53, 18, 8, 11, 47] also rely on supervised learning and historical data, which makes the research more suitable for post-event analysis rather than early-stage intent prediction.

Notably, the author [15] presents the research most relevant to our work, which evaluates co-orbital threats by propagating the orbits of both satellites, scanning all possible departure times and TOF, and solving Lambert transfers to compute the required Δv using genetic algorithms (GA). The computed Δv is then compared with the pursuer's Δv budget to determine whether interception is possible within the evaluation window. The study presents key findings and bears some similarity to our research. However, our research searches all possible TOFs instead of Δv . One reason that we pick the TOF instead of Δv is that without knowing the specific Δv threshold of the counterpart satellite, it is difficult to establish a meaningful threshold and use it as an alert strategy for Blue. Therefore, TOF is a more meaningful and realistic metric for detecting intent. Moreover, rather than applying a simple threshold, one shortcoming is that the author [15] does not address the level of intent; given the complexity and unknown factors of each satellite's Δv , several practical questions remain unclear for this work. In Section 5, we specifically discussed that our model's robustness across different values of Δv limit. Fewer similar studies that infer Δv or combine GA methods with the Lambert problem can be found in [52, 41, 29, 3]. Similarly, there is no classification or follow-up after the Δv is computed, though these approaches could be a valuable resource in the future for maneuver classification.

Some studies utilize methods other than the Lambert solver. For example, this paper [36] investigates maintaining catalogs of Resident Space Objects (RSOs) by testing possible maneuver epochs over a search window, applying either a single-burn or a two-burn hypothesis, and checking whether the resulting trajectory matches the post-maneuver observations. Instead of using a classical Lambert solver, the authors employ a linearized dynamics approach, which is computationally efficient in this case. In future research, alternatives to the Lambert solver could be considered for integration with our game-theoretic model.

Additional information and research that could enhance future intent detection can be found in [32], which proposes a method for associating orbital tracks between two objects by applying the Lambert problem. While the primary focus is on tracklet association, the method may also provide indirect evidence of maneuvers in cases where observed trajectories cannot be linked to a common object using the Lambert solution.

Finally, while many studies focus on machine learning methods, few utilize game theory to classify satellite maneuver intent. The most relevant work is paper [40], which employs a game-theoretic pursuit–evasion model to design and modify orbital transfers based on real satellite data. The generated trajectories are then used to train and test a CNN that categorizes different types of satellite maneuvers. However, the model's accuracy when confronted with real hostile-intent maneuvers remains unclear.

As the related work shows, many researchers focus on monitoring and detecting anomalous satellite behaviors to better prevent or evade such threats. However, a critical gap remains: how can we detect adversarial intent automatically at the earliest possible stage with incoming TLE data, while relying on as little trajectory information as possible, even before maneuvers become overtly threatening? These limitations motivate our work, which focuses on investigating automated approaches for early-stage threat identification and intent inference.

3. PROPOSED GAME MODEL

In this paper, we propose a novel game-theoretic formulation which models the interaction between a defending satellite operator (“Blue”) and a potentially-attacking satellite operator (“Red”). While this has many similarities to classical pursuit-evasion games (see [50] and references therein for an overview), existing models do not capture several key features that this strategic interaction requires. In a classical pursuit-evasion game, an evader (E) attempts to maneuver to outrun a pursuer (P). The identities of E and P are known to both agents and fixed throughout the interaction, so the main strategic questions center on characterizing the sets of initial conditions which can guarantee that P is able to capture E.

In contrast, orbital interactions between nation-states need not involve clearly defined and permanently fixed roles. In peacetime, there is neither an evader nor a pursuer: while either nation may deploy ASAT weapon systems on orbit during peacetime, these systems' capabilities and targets may be only vaguely known to the other nation. However, if a war between the two is initiated, Red's orbital ASAT weapons suddenly become “pursuers” and Blue's orbital surveillance platforms suddenly become “evaders.” This change of roles may occur without notice to satellite operators of either nation; for reasons of operational security, even Red's satellite operators may not be told that war is imminent

until the last minute. That is, both Red and Blue have *partial information* regarding a fundamental aspect of the interaction. Finally, an *informational asymmetry* may be present if the war is initiated as a “sneak attack”: Red’s satellite operators may know about the role change *before* Blue’s operators do.

Accordingly, this paper poses a new differential game formulation which captures several elements relevant to this strategic interaction. Specifically, our novel model is indexed by time t and allows for

- **A role-change** which occurs at *trigger time* T_A ; at all pre- T_A times $t < T_A$, Red is not pursuing Blue. At all post- T_A times $t \geq T_A$, Red and Blue are engaged in a pursuit-evasion game in which Red is the pursuer and Blue is the evader.
- **Partial information:** Red does not know in advance when T_A will occur; however, after T_A has passed, Red can observe this fact.
- **Informational asymmetry:** Even after T_A has passed, this fact is never explicitly revealed to Blue. If Blue wishes to know that $t > T_A$ (i.e., T_A has passed), they must infer this fact from Red’s observed behavior.

We are not aware of any existing game formulations that include this time-dependent adversarial interaction; thus, we believe this model is poised to have substantial impacts in differential game theory, even beyond the specific orbital game which we envision here.

3.1 Satellite Behavior Models: What Red and Blue Do

First, we will describe the *behavior* of the satellites; then we will describe the potential strategies which the satellite operators may employ. Throughout, our envisioned threat model is that the Red satellite is a kinetic kill vehicle (KKV); however, many of the fundamental principles can be adapted to a variety of other threat models.

We assume that both satellites begin in arbitrary orbits, and that as time t advances, Red may perform impulsive maneuvers (subject to reasonable constraints). To narrow our focus on Blue’s problem of inferring intent by observing Red’s maneuvers, we assume that Blue never maneuvers but simply coasts under natural forces.

3.1.1 Red’s Behavior Model: Impulsive Maneuvers

We assume that Red can execute arbitrary (but limited) impulsive maneuvers, subject to a rate constraint (to model its maximum specific impulse) and a constraint on total ΔV across all maneuvers (to model its limited fuel reserves). Mathematically, these constraints are modeled in the following way.

Throughout the course of an interaction, suppose Red takes m impulsive maneuvers at times $T = \{t_1, t_2, \dots, t_m\}$, so that the collection of impulses is $\{I_k\}_{k \in T}$ where each impulse I_k is expressed in m/s in a suitable coordinate frame, e.g., $I_k = (i_{x,k}, i_{y,k}, i_{z,k})$. If Red applies impulse I_k at time t_k , this causes an instantaneous step change in Red’s velocity at time t_k . The magnitude of each impulse I_k is its Euclidean norm $\|I_k\|$, and the sum of these magnitudes is constrained:

$$\sum_{k \in T} \|I_k\| \leq B_R \quad (1)$$

where B_R represents Red’s total fuel reserves and is expressed in m/s. In addition, Red cannot impulse too much too often (to model limits on a spacecraft’s maximum thrust). To model this, given a duration W and an impulse upper bound \bar{I} , we require for all times t that

$$\sum_{t_k \in [t, t+W]} I_k \leq \bar{I}. \quad (2)$$

Thus, over any time window of duration W , Red cannot expend more than \bar{I} total Δv .

3.1.2 Blue’s Behavior Model: Alerting to Hostile Red Maneuvers

Red’s goal is to destroy Blue soon after T_A ; Blue’s goal is to survive as long as possible after T_A . In a real scenario, if Red telegraphs the intent too obviously, Blue has a good chance of evasion. We model this by giving Blue a binary “alert” decision variable, which is costly to “turn on” but which decreases Red’s chances of a successful kill while

active. We interpret the “alert” abstractly; conceptually, we might think of the alert as corresponding to “taking evasive maneuvers” or something similar.¹ In our formulation, an alert decreases Red’s chance of a successful kill the longer it remains on.

We model Blue’s alert status over time using the function $A(t)$, where

$$A(t) = \begin{cases} 1, & \text{if Blue is on alert at time } t, \\ 0, & \text{if Blue is not on alert at time } t. \end{cases} \quad (3)$$

Blue has a constraint (a “budget”) on the total amount of time A can be active:

$$\int_0^{\infty} A(t) dt \leq B_B$$

Hence, trivial and physically meaningless strategies such as “remain on alert all the time” are not possible.

3.2 Satellite Operator Strategies: What Red and Blue *Decide*

In a differential game, each player competes by pre-computing a plan, called a *policy* or a *strategy*. Each player’s strategy is a function which inputs the history of play up to the current time, and outputs behavior actions to perform. Here, we consider various strategic concerns formally; first for Red, then for Blue.

3.2.1 Red’s Strategies: Deciding when to maneuver

A Red strategy is a function which looks at all the game’s history up to time t (i.e., full state trajectories of both satellites, all previous Red maneuvers, all previous Blue alert states) and then decides on an impulsive maneuver (or lack thereof) at time t . For example, a naive strategy might say “station-keep close to Blue when $t < T_A$, and then move aggressively to intercept immediately after T_A passes.” Again, the strategy space is enormous and we leave its full characterization to future work. Nonetheless, here we suggest several ways that Red might notionally organize its strategies.

- After T_A , Red wants to give Blue as little time to react as it possibly can. However, this *need not* mean that Red will immediately make an aggressive move. Red might instead make a benign-looking move which gives it an opportunity to strike aggressively at some time soon in the future.
- Before T_A , Red has the option to try to induce false alerts in an effort to make Blue waste its alert budget (e.g., run out of fuel for evasion). We believe that this potential for deception holds great promise for interesting behavior.
- Finally, it is likely in Red’s interest to behave almost exactly the same when $t < T_A$ as when $t \geq T_A$. If Red immediately maneuvers when T_A occurs, then Blue should be able to see the change and know that T_A has passed.

3.2.2 Blue’s Strategies: Deciding when to alert

Similarly, a Blue strategy is a function which looks at all the game’s history up to time t and then decides on an alert state for time t . The space of feasible strategies is thus enormous. For instance, Blue could organize its strategies using a taxonomy like the following:

- “0th-order:” Blue alerts if Red is within a certain radius.
- “1st-order:” Blue alerts if Red’s current trajectory intersects with Blue’s at some point in the near future.
- “2nd-order:” Blue alerts if Red’s current trajectory gives Red a future opportunity to be on a short collision course (i.e., 2nd-order means that Blue projects Red’s future opportunities to attack without warning).

¹Future iterations can explicitly model evasion; however, our perspective is that this abstract “alert” model captures the core strategic elements while keeping the model reasonably simple.

Here, we provide parameterized reference instantiations of each of these classes of strategies.

0th-Order Strategy: Distance-Based Alerting

Blue activates alert mode whenever Red is within a given distance d_{thresh} :

$$A(t) = \begin{cases} 1, & \text{if } \|\mathbf{x}_R(t) - \mathbf{x}_B(t)\| \leq d_{\text{thresh}}, \\ 0, & \text{otherwise.} \end{cases}$$

where $\mathbf{x}_R(t)$ is Red's position, \mathbf{x}_B is Blue's position, and d_{thresh} is the distance threshold for alert activation.

1st-Order Strategy: Collision Course Alerting

Blue activates alert mode if Red's current orbit will result in a collision with Blue within time T_{max} :

$$A(t) = \begin{cases} 1, & \text{if } \exists \tau \in [0, T_{\text{max}}] \text{ such that } \|\mathbf{x}_R^{\text{pred}}(t + \tau) - \mathbf{x}_B^{\text{pred}}(t + \tau)\| \leq \varepsilon, \\ 0, & \text{otherwise.} \end{cases} \quad (4)$$

where $\mathbf{x}_R^{\text{pred}}(t + \tau)$ and $\mathbf{x}_B^{\text{pred}}(t + \tau)$ are Red's and Blue's predicted positions at time τ under the influence of natural forces (computed using an appropriate orbit propagator) and ε is an appropriate distance around Blue.

2nd-Order Strategies: Monitor Future Opportunities for Collision

This strategy evaluates how soon Red could collide with Blue, given a future maneuver by Red. Here, Blue monitors Red's potential future "terminal" maneuvers. In other words, suppose that Red makes a single impulsive maneuver I_k at time $t_k \geq t$ which results in an eventual collision at time $T_C(I_k)$. We define the *minimum time-to-collision function*:

$$T_{\min}(t) = \min_{\substack{I_k \text{ feasible} \\ t_k \geq 0}} \left\{ T_C(I_k) - t_k \mid \mathbf{x}_R^{\text{pred}}(T_C(I_k), t_k; I_k) = \mathbf{x}_B^{\text{pred}}(T_C(I_k)) \right\} \quad (5)$$

where:

- $\mathbf{x}_R^{\text{pred}}(t, t_k; I_k)$ is Red's predicted position at time t given impulsive maneuver I_k executed at time t_k ,
- $\mathbf{x}_B^{\text{pred}}(t)$ is Blue's predicted position at time t , and
- The minimization is taken over all feasible maneuvers I_k that Red can execute under its impulse constraints.

This approach allows Blue to continuously track the evolving threat of a collision and react accordingly. Note that a 1st-order policy can easily be derived from $T_{\min}(t)$; whenever $T_{\min}(t) = 0$, this means that Red is on a collision course with Blue.

Table 1 provides a very simple comparison of these 3 strategic options.

Strategy	Trigger Condition	Pros	Cons
0th-Order	Distance to Red	Simple, fast	Easily tricked
1st-Order	Predicted collision	Smarter, less wasteful	Still short-term
2nd-Order	Future opportunity	Best defense	Computationally heavy

Table 1: Comparison of Blue's parameterized strategies.

While this framework is instructive, it is likely that *optimal* Blue strategies could be considerably more complicated. For instance, none of these strategies meaningfully consider the history of interactions, which could be very useful information (e.g., Blue could estimate Red's remaining fuel reserves). In a real operational scenario, Blue would likely use a mix-and-match approach (potentially involving randomization to induce uncertainty in Red). In Section 4, we propose a specific 2nd-order alert strategy based on solutions to Lambert's problem. In Section 5, we extensively explore this alert strategy using real orbital data and validate it against historical ISS resupply missions.

3.3 Knowledge Assumptions: Who knows what, and when?

In the interest of model simplicity and analytical tractability, we make permissive knowledge assumptions. Red and Blue both know:

- Positions and velocities of Red and Blue. This is a necessary assumption for the basic well-posedness of the game model; however, even our proposed 2nd-order alert method which we describe in Section 4 does not require full positions and velocities (or even precise maneuver information), and instead infers intent merely by monitoring TLE updates.
- Complete strategies of Red and Blue. Again, this is a standard assumption in game-theoretic work that initially appears overly generous; however, it is actually grounded in the concept that both Red and Blue can perform actions which “probe” each others’ responses, and in so doing learn a great deal about each others’ strategies.

The only informational asymmetry is with regard to the trigger time T_A :

- Blue has no knowledge of T_A other than what it can infer from Red’s behavior.
- Red has no knowledge of *when* T_A will occur, but knows T_A after it passes.

3.4 Stackelberg Equilibrium Model

We model this as a game in which Blue pre-commits to a strategy (an alert policy), and Red selects a strategy (maneuver policy) to maximize its payoff in response to Blue’s alert policy. This leader/follower structure is known as a Stackelberg game and has been the basis of some of the most successful applied game theory in the context of security planning [43, 28, 35].

3.5 The Game’s Cost Functions

In order to form the above primitives into a mathematically well-posed game, cost functions must be defined which guide Red’s and Blue’s strategy choices. Here, we propose a reference set of cost functions for Red and Blue.

3.5.1 Effect of Alert

We define the function $M(t;A)$ to measure the way that Blue’s recent alert status decreases Red’s chance of a successful kill. Mathematically, $M(t;A)$ represents the probability of a successful kill at time t given Blue’s recent alert status. There are several possible ways to formulate this function; two potential examples are presented here.

Windowed Average: Let $\beta > 0$ be a constant parameter that represents a time duration; the probability of a successful kill at time t is equal to the fraction of the past β time-units during which Blue’s alert was not active. Mathematically, we have

$$M(t;A) = \frac{1}{\beta} \int_{t-\beta}^t (1 - A(\tau)) d\tau. \quad (6)$$

This means that if Blue has been continuously on alert for β time-units, the probability of a successful kill drops to 0; if Blue has been continuously on alert for $\beta/2$ time-units, the probability of a kill is $1/2$.

Linear decay, instant reset: Let $\alpha > 0$ be a constant parameter. Suppose that at time t , $A(t) = 1$, and it has been continuously 1 since time τ . Then we define²

$$M(t;A) = \max \{0, 1 - \alpha[t - \tau]\},$$

where $(t - \tau) \geq 0$. Thus, the longer Blue remains continuously on alert, the smaller $M(t;A)$ becomes, down to 0. In this formulation, if the alert is on continuously for $1/\alpha$ time units, then the probability of a kill goes to 0.

If $A(t) = 0$ (i.e., Blue is not on alert at time t), then we set

$$M(t;A) = 1.$$

In other words, as soon as Blue goes off alert, the function resets to its full value of 1. However, if Blue switches alert on again at a later time, the clock $(t - \tau)$ restarts from that new on-switch moment.

²Note that we could choose any functional form for $M(t;A)$ which is decreasing in $t - \tau$.

3.5.2 Red's Penalty for Parking Next to Blue

One trivial strategy which Red could employ is to “park” very close to Blue when $t < T_A$, depleting Blue's alert budget long before T_A passes. However, this strategy is typically not employed in real satellite interactions; we conjecture that this is because nation-states have political incentives *not* to unnecessarily inflame geopolitical tensions. As a proxy for these political incentives, our model penalizes Red for parking too close to Blue.

Here, we present one possible mathematical formulation of this penalty. Let $\delta > 0$ captures the aggressiveness of the penalty, and define

$$\tilde{P}(t) = \int_0^t e^{-\delta \cdot \|x_R(\tau) - x_B(\tau)\|} d\tau \quad (7)$$

Thus, $\tilde{P}(t)$ is a measure of cumulative distance between Red and Blue over the interaction's timeline, weighted by distance: very small distances significantly increase the value of $\tilde{P}(t)$. Then $P(t)$ represents the penalty for Red being too close to Blue for too long before a collision occurs:

$$P(t) = e^{-\tilde{P}(t)} \quad (8)$$

Since $\tilde{P}(t) \geq 0$, we always have that $P(t) \in [0, 1]$ so that it can be interpreted as a probability.

3.5.3 Red's Objective

Red's objective is to destroy Blue quickly after T_A . This has 3 parts:

1. Red and Blue's location coincide at some time (i.e., Red and Blue collide).
2. Blue has not been on alert for “too long” prior to that collision (i.e., $M(t; A)$ is still nonzero).
3. Not too much time has passed since T_A .

Let $C(t)$ be an indicator function for a collision having happened in the past:

$$C(t) = \begin{cases} 1, & \text{if Red and Blue have collided at some time } \tau \leq t, \\ 0, & \text{otherwise.} \end{cases}$$

Define $T_C := \min\{t : C(t) = 1\}$ as the first time of collision. To promote urgency in Red's behavior, define a function $D(t; T_A)$ (parameterized by time constant $\gamma > 0$) which expresses the multiplicative penalty Red experiences when Blue is destroyed at time $t \geq T_A$:

$$D(t; T_A) = e^{-(t-T_A)\gamma}. \quad (9)$$

We then define Red's payoff as

$$U_R(\{I_k\}, A) := \begin{cases} C(T_C)M(T_C; A)D(T_C; T_A)P(T_C) & \text{if } T_C \geq T_A, \\ 0 & \text{otherwise.} \end{cases}$$

That is, Red wants a collision ($C(T_C)$), wants Blue *not to be alerting* ($M(T_C; A)$), wants the collision to happen soon after T_A ($D(T_C; T_A)$), and does not want to accrue a large parking penalty ($P(T_C)$).

3.5.4 Blue's Objective

Blue's objective is to avoid being destroyed, leading to the following cost function:

$$U_B(\{I_k\}, A) := -C(T_C)M(T_C; A)D(T_C; T_A).$$

That is, Blue does not want a collision ($C(T_C)$), wants to be alerting ($M(T_C; A)$), and wants any collision to happen *long* after T_A ($D(T_C; T_A)$).

4. LAMBERT'S PROBLEM-BASED 2ND-ORDER ALERTING

Having posed the game model in Section 3, here we present a specific design for a 2nd-order alerting strategy that is designed to monitor the earliest possible collision risk between a defending satellite (Blue) and a potential attacker (Red), under the assumption that Red may execute an optimal impulsive maneuver at any point in the near future. First, we review Lambert's problem; we then proceed to describe the alerting technique.

4.1 Lambert's Problem

Lambert's problem is a classical boundary-value problem in astrodynamics. Given two position vectors \mathbf{x}_1 and \mathbf{x}_2 and a time-of-flight Δt , Lambert's problem is the problem of finding a Keplerian orbit that connects these points within the specified time. Thus, we write an instance of Lambert's problem as $(\mathbf{x}_1, \mathbf{x}_2, \Delta t)$, and a solution of Lambert's problem is a pair of velocity vectors $(\mathbf{v}_1, \mathbf{v}_2)$ (which we call the *departure* and *arrival* velocities) such that an orbiting body with initial state $(\mathbf{r}_1, \mathbf{v}_1)$ will arrive at final state $(\mathbf{r}_2, \mathbf{v}_2)$ after an elapsed time of Δt . Due to its centrality in practical problems of orbital rendezvous, much work has focused on determining solutions to Lambert's problem numerically [7, 6, 20], and our work can leverage these approaches. For more details on Lambert's problem, including applications, algorithms, and other considerations, the interested reader may refer to [48].

In our work, we use Lambert transfers as a proxy for short-duration kinetic attacks; we call these *Lambert attacks*. By computing the change in velocity (Δv) required to execute such a maneuver and comparing that against a hypothetical Δv budget for Red, Blue can estimate the minimum time-of-flight in which Red could rendezvous with Blue (i.e., execute a kinetic attack). Here, we mathematically describe our approach in detail. Suppose that at time t_0 , the orbital positions and velocities of Blue and Red are $(\mathbf{x}_B(t_0), \mathbf{v}_B(t_0))$ and $(\mathbf{x}_R(t_0), \mathbf{v}_R(t_0))$, respectively. For $t \geq t_0$, let $(\mathbf{x}_B(t), \mathbf{v}_B(t))$ and $(\mathbf{x}_R(t), \mathbf{v}_R(t))$ denote the projected positions and velocities of Blue and Red (respectively) as calculated by an appropriate orbit propagator.

For $t' > t \geq t_0$, let $\mathbf{v}_2(t, t')$ denote the *departure* solution to Lambert's problem $(\mathbf{x}_R(t), \mathbf{x}_B(t'), t' - t)$. That is, an orbiting body with initial state $(\mathbf{x}_R(t), \mathbf{v}_2(t, t'))$ will arrive at final position $\mathbf{x}_B(t')$ at time t' . In words, if Red waits until time t , then impulsively changes its velocity to $\mathbf{v}_2(t, t')$, it will intercept Blue at time t' . To do this, Red needs to apply an impulsive maneuver of $\Delta \mathbf{v}_R(t, t') := \mathbf{v}_2(t, t') - \mathbf{v}_R(t)$.

Suppose that Blue wishes to perform a hostility assessment over the time window $[t_0, t_0 + T]$ for some horizon length $T > 0$. In this context, Blue will compute the minimum time-of-flight Lambert attacks which will be possible in the time window under consideration, given some estimated Red Δv budget \bar{v} . That is, at time t , Blue wishes to compute

$$T_{\min}(t_0) := \min_{t' \geq t_0} \{t' - t : \|\Delta \mathbf{v}_R(t, t')\| \leq \bar{v}\}. \quad (10)$$

The function $T_{\min}(t_0)$ returns the minimum time-of-flight of any Lambert attack that Red can perform in the time window $[t_0, t_0 + T]$ which require an impulse less than \bar{v} . Thus, $T_{\min}(t_0)$ can be used to estimate the value of Red's strategic positioning: if the value of the function is very low, this means Red has significant attack opportunities in the near future; if the value of this function is high, this means that Red lacks good near-future opportunities.

4.2 2nd-Order Alerting Approach

In this paper, our goal is to use this function to assess potential hostile intent in observed Red maneuvers using minimal orbital data. To this end, suppose that a new Red TLE (we call this the *post* TLE) update is received at time t_0 and the previous Red TLE (we call this the *pre* TLE) was seen at time t_- . If Blue suspects that Red has performed a hostile maneuver between time t_- and t_0 , it can do the following.

First, compute $T_{\min}^{\text{pre}} := T_{\min}(t_0)$, using Red's *pre* TLE to seed the orbit propagator which is used to compute $\Delta \mathbf{v}_R(t, t')$ in (10). That is, T_{\min}^{pre} represents the shortest-duration attack that was possible in the $[t_0, t_0 + T]$ time window *before* Red's maneuver was executed. Note that T_{\min}^{pre} is a counterfactual in the sense that it captures the strategic position that Red would have had, if Red had not maneuvered.

Second, compute $T_{\min}^{\text{post}} := T_{\min}(t_0)$, using Red's *post* TLE to seed the orbit propagator in (10). That is, T_{\min}^{post} represents the shortest-duration attack that is now possible in the $[t_0, t_0 + T]$ time window *after* Red's maneuver was executed. Thus, we can view T_{\min}^{post} as a direct measurement of Red's actual strategic position as of time t_0 .

These two computed times-of-flight T_{\min}^{pre} and T_{\min}^{post} can then be compared to assess the aggregate "hostility" of any maneuvers which Red performed between times t_- and t_0 . If $T_{\min}^{\text{pre}} = T_{\min}^{\text{post}}$, this indicates that Red's strategic position is

unchanged from t_- to t_0 (at least from the standpoint of the duration of Lambert attacks). If $T_{\min}^{\text{pre}} > T_{\min}^{\text{post}}$, this indicates that Red’s strategic position has improved. Conceptually, there are many possible ways to quantitatively capture this comparison. Here, we propose to use the following *intent score* metric:

$$\text{Intent} = \frac{T_{\min}^{\text{pre}}}{T_{\min}^{\text{pre}} + T_{\min}^{\text{post}}}. \quad (11)$$

Equation (11) allows a straightforward and uniform means of measuring intent, since it succinctly summarizes changes in Red’s strategic position. There are 3 possibilities:

- **Intent close to 1:** T_{\min}^{post} is much smaller than T_{\min}^{pre} , which means that Red executed a maneuver which significantly improved its strategic positioning.
- **Intent close to 0:** T_{\min}^{post} is much larger than T_{\min}^{pre} , which means that Red executed a maneuver which significantly degraded its strategic positioning.
- **Intent = 0.5:** T_{\min}^{post} is equal to T_{\min}^{pre} , which means that even if Red executed a maneuver, it does not result in any strategic changes.

With this proposed method of assessing maneuver intent in hand, we proceed in Section 5 to present the results of our validation experiments.

5. EMPIRICAL RESULTS

This study incorporates three datasets representing distinct real-world satellite interaction scenarios. The first case involves Japan’s HTV-1 (modeled as Red) resupply mission to the ISS (modeled as Blue) in September 2009, along with its published maneuver events. These events are used to verify our intent score. The second dataset tracks the U.S. reconnaissance satellite USA-245 (modeled as Blue) and Russian satellites Kosmos 2542/2543 (modeled as Red) from late 2019 through mid 2020, demonstrating possible close-range orbital proximity operations. The third example features geostationary (GEO) orbital movement involving China’s SJ-21 (modeled as Blue) and SJ-25 (modeled as Red), highlighting proximity operations in GEO.

5.1 ISS (Blue) and HTV-1 Cargo Spacecraft (Red)

We first examine the HTV-1 resupply mission to the International Space Station (ISS), highlighting key phases from launch through docking. The Japan Aerospace Exploration Agency (JAXA) launched the H-II Transfer Vehicle-1 (HTV-1), a cargo delivery spacecraft to the ISS [34].

This section analyzes the intent score in conjunction with published HTV-1 events, including height adjustment maneuvers (HAMs), arrival 5 km behind the ISS Approach Initiation (AI) point, and capture by the ISS robotic arm (SSRMS).³ The time and maneuvers are documented in Table 2. The maneuver and docking events can be found at [23, 21, 22, 34].

Event	Time
Height Adjustment Maneuver 1	09/16/2009 12:04 am
Height Adjustment Maneuver 0	09/17/2009 9:24 am
Height Adjustment Maneuver 3	09/17/2009 12:26 pm
5 km behind the ISS AI point	09/17/2009 1:59 pm
Captured by the station’s robotic arm	09/17/2009 7:51 pm

Table 2: HTV-1 key maneuver events

In this paper, we define the upper limit of ΔV as 500 m/s; therefore, the TOF is subject to this constraint. Note that in all graphs, only intent scores greater than 0.5 are included. An intent score close to 1 indicates a significant decrease

³All timestamps have been converted from Japan Standard Time to Coordinated Universal Time, UTC

Index	Timestamp (UTC)	Intent Score
1	09/15/2009 10:21 am	0.52
2	09/15/2009 5:24 pm	0.56
3	09/16/2009 2:43 am	0.63
4	09/17/2009 3:00 am	0.67
5	09/17/2009 6:08 pm	0.96

Table 3: HTV-1 intent score with timestamp. The table lists the times of intent score generation as well as the corresponding intent score values. Results are shown with ΔV limited to 500 m/s; only intent scores above 0.5 are included. Scores near 1 indicate a high likelihood of hostile maneuvers, 0.5 indicates no change, and scores near 0 indicate a reduced likelihood. See Figure 1, scores at indices 1–5 are highlighted in red at the top of the graph.

in the minimum TOF, suggesting a high likelihood of a hostile maneuver. An intent score of 0.5 indicates no change, while an intent score close to 0 indicates a significant increase in the minimum TOF. The intent score is calculated at each epoch obtained from TLE, not immediately after each maneuver. After HAM0, HAM3, and the approach from behind the ISS at the AI point, the next TLE update comes in, and our intent score which is calculated immediately based on the incoming TLE data shows a sharp rise to 0.96. This demonstrates that our method successfully detects intentional maneuvers and captures their significance when one satellite approaches another. As shown in Figure 1, after 09/17/2009, the distance between the two objects remains low, making it difficult to distinguish changes visually. Even though the geospatial differences are subtle, our method still identifies the critical change and alerts the system that one satellite is approaching the other.

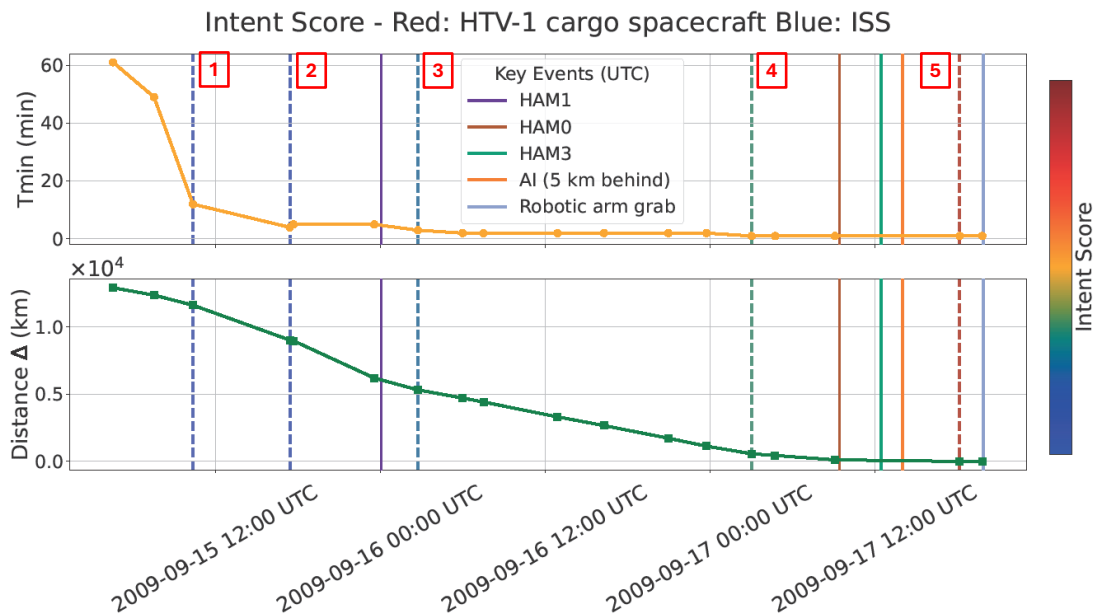


Fig. 1: The top subplot shows the minimum time-to-collision, T_{\min} , and the bottom subplot shows the distance difference between Red and Blue. Vertical dashed lines indicate the intent score, with lower scores shown in blue and higher scores in red; the score is scaled from 0 to 1. In this paper, we define the upper limit of ΔV as 500 m/s, and thus the TOF is subject to this constraint. The figure only shows intent scores greater than 0.5. The solid lines mark planned orbital burns and the final docking. The legend in the middle identifies key maneuver events documented on the JAXA website. The intent score at index 3, immediately after the first height adjustment, is 0.63. After three consecutive maneuvers, the intent score at index 5 rises significantly, reaching 0.96, as indicated by the red dashed line. Intent score indices are labeled at the top of the graph. The specific values of intent scores 1–5 are listed in Table 3.

The following heat maps Figure 2, Figure 3, and Figure 4, show the Time of Maneuver (TOM) vs. TOF for intent

Index-3 Heatmap of HTV Scores

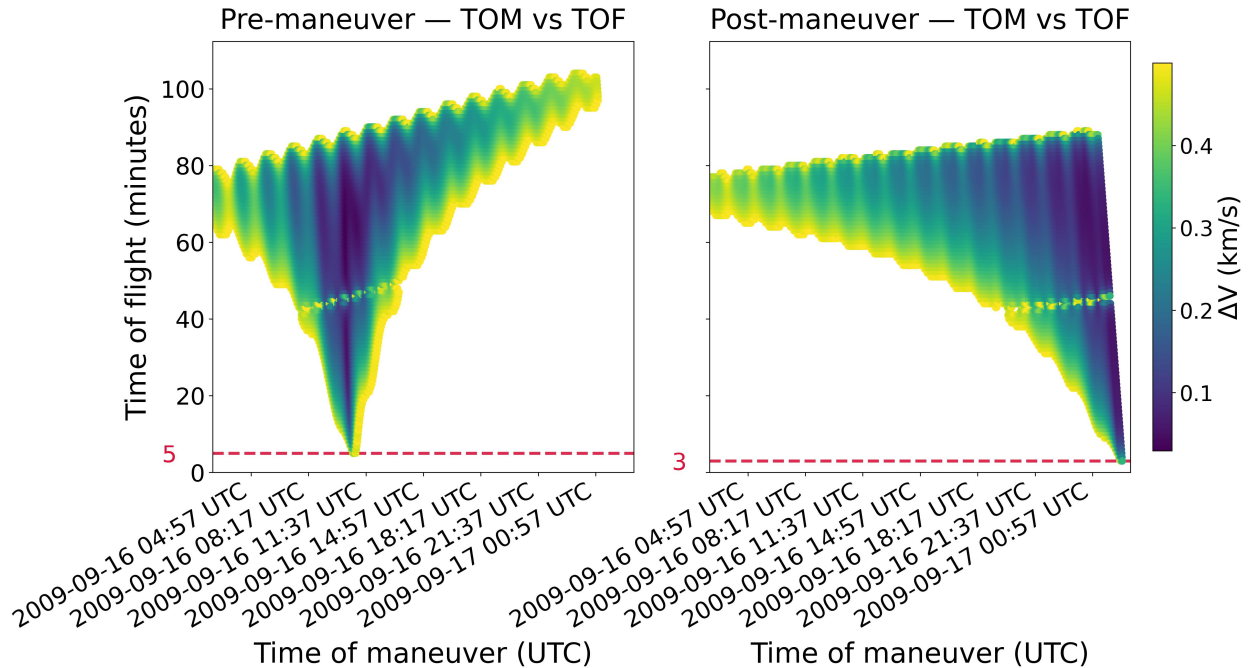


Fig. 2: Heat map of the HTV-1 intent analysis at intent score index 3; see the score indices in Figure 1 and Table 3. The intent score is 0.63. Red T_{min} before the maneuver is 5 minutes, and Red T_{min} after the maneuver is 3 minutes. The graphs represent the future T_{min} for Red if both Red and Blue are propagated at the same time. Both plots show the possible TOF for Red to intercept Blue within a one-day range. The color bar indicates the coordinate ΔV required to achieve the corresponding TOF at the maneuver time. The left graph shows T_{min} assuming Red performs no maneuvers (the previous state), while the right graph shows T_{min} after the maneuver.

scores at index 3, 4, 5 of the HTV-1 rendezvous with the ISS. Specifically, the heat maps show the possible TOF for Red to intersect Blue within the one-day orbit propagation range, with the ΔV upper limit set to 500 m/s.

For each Red TLE list, we sort both the Red and Blue TLEs in ascending order by epoch time. For each Blue TLE, two consecutive Red TLEs are paired such that the Blue TLE epoch lies after the first Red TLE epoch (referred to as Pre-maneuver in Figure 2, Figure 3, and Figure 4) but before the second Red TLE epoch (referred to as Post-maneuver in Figure 2, Figure 3, and Figure 4). All orbit propagation times are aligned with the epoch of the Post-Red TLE. Any intentional maneuvers of Red to approach Blue that occur between the Red pre-TLE and post-TLE will result in a significant drop in the TOF on the Post-maneuver graph.

The x-axis in Figure 2, Figure 3, and Figure 4 represents the orbital propagation time starting from the Post-maneuver Red TLE epoch. The y-axis represents the TOF until Red intersects with Blue. The color bar represents the ΔV required by Red to perform the corresponding maneuvers to intersect Blue.

Figure 2 shows the corresponding heat maps immediately after HAM1. Before the maneuver, the minimum T_{min} decreases to 5 minutes around 2009/09/16 11:37 and then increases again, indicating that no meaningful maneuvers after that time could enable a faster approach to the ISS. In addition, at every possible minimum TOF, the required ΔV is very high, which also implies that no easy maneuvers were available. However, after the HAM1, the minimum TOF decreases as the orbit propagates and continues to decrease over time to 3 minutes at the end of the propagation window. Notably, toward the end, the ΔV required to reach the minimum TOF also drops. This means that HAM1 created a significant opportunity for HTV-1 to approach the ISS in the future.

Figure 3 shows the corresponding heat maps at intent score index 4. No publicly documented maneuvers of HTV-1 occurred after HAM1. The heat maps also show the same trend: the chance of obtaining a minimum TOF does not significantly or continuously decrease with orbital propagation between the pre-maneuver and the post-maneuver. This

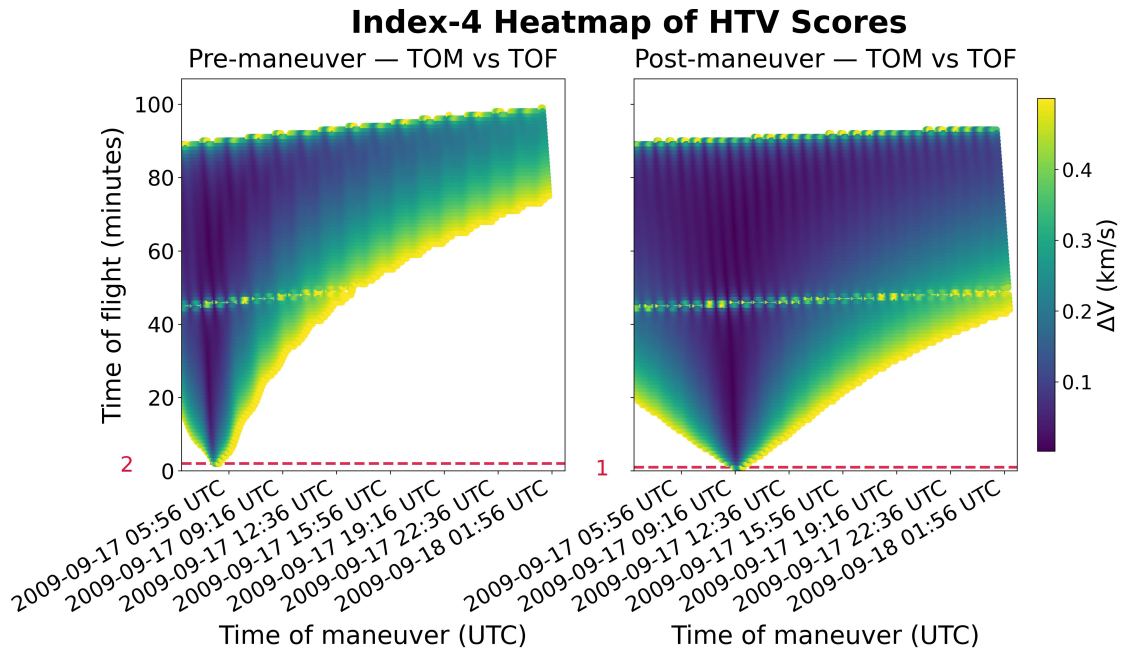


Fig. 3: Heat map of the HTV-1 intent analysis at intent score index 4; see the score indices in Figure 1 and Table 3. The intent score is 0.67. Red T_{min} before the maneuver is 2 minutes, and Red T_{min} after the maneuver is 1 minute. The graphs represent the future T_{min} for Red if both Red and Blue are propagated at the same time. Both plots show the possible TOF for Red to intercept Blue within a one-day range. The color bar indicates the coordinate ΔV required to achieve the corresponding TOF at the maneuver time. The left graph shows T_{min} assuming Red performs no maneuvers (the previous state), while the right graph shows T_{min} after the maneuver. TOF of pre-manuever and post-manuever show a similar trend.

aligns well with our intent score of 0.67, where no significant hostile intent is detected.

Figure 4 shows the heat map after three maneuver events (HAM0, HAM3, and arrival at 5 km behind the ISS AI point). The post-manuever heat map indicates the optimal TOF across the entire orbital propagation with low ΔV compare to pre-manuever heat map. This provides evidence that our system can detect maneuvers intended to approach another satellite, which result in a minimum TOF in the future.

To demonstrate that our model generalizes to various unknown ΔV values, we plot the intent score against different ΔV limits ranging from 100 to 1,000 m/s. Figure 5 shows the intent scores at indices 3, 4, and 5 under different ΔV limits. As Figure 5 shows, the intent score at index 3 remains steadily above 0.6, while the intent score at index 4 drops to the lower control limit of 0.5 after 800 m/s, which will require further investigation in our future work. The intent score at index 5 remains consistently above 0.9. This result suggests that, even without prior knowledge of the ΔV limit of the pursuer satellite, our system can still capture and alert the intent.

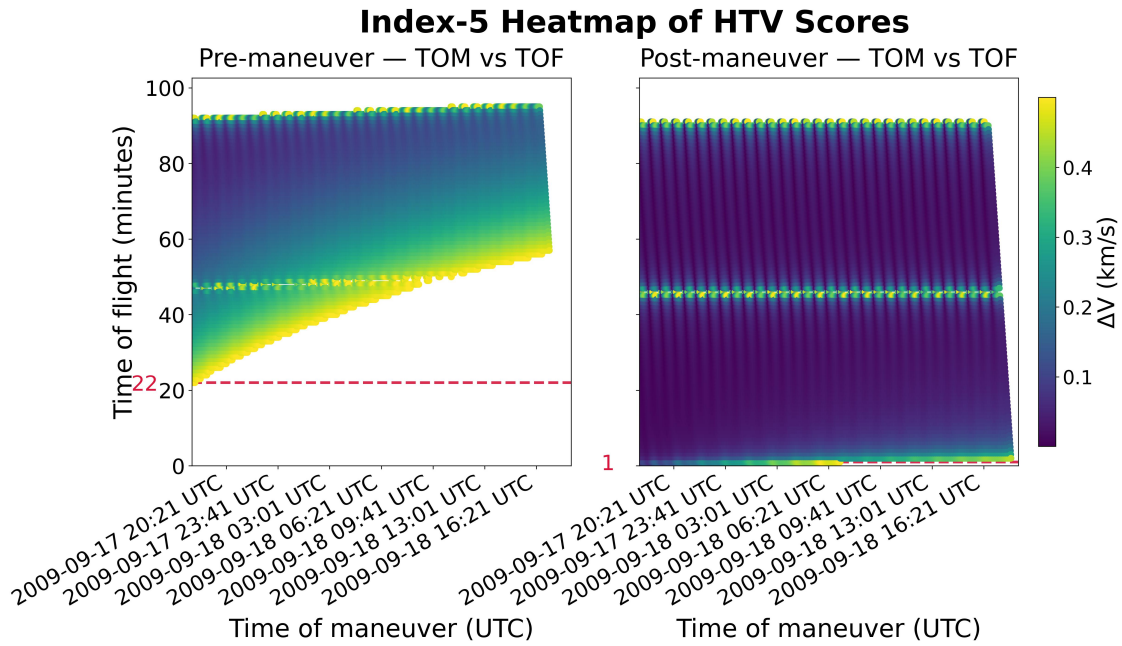


Fig. 4: Heat map of the HTV-1 intent analysis at intent score index 5; see the score indices in Figure 1 and Table 3. The intent score is 0.96, indicating a very high-intent maneuver. Red T_{\min} before the maneuver is 22 minutes, and Red T_{\min} after the maneuver is 1 minute. The graphs represent the future T_{\min} for Red if both Red and Blue are propagated at the same time. Both plots show the possible TOF for Red to intercept Blue within a one-day range. The color bar indicates the coordinate ΔV required to achieve the corresponding TOF at the maneuver time. The left graph shows T_{\min} assuming Red performs no maneuvers (the previous state), while the right graph shows T_{\min} after the maneuver.

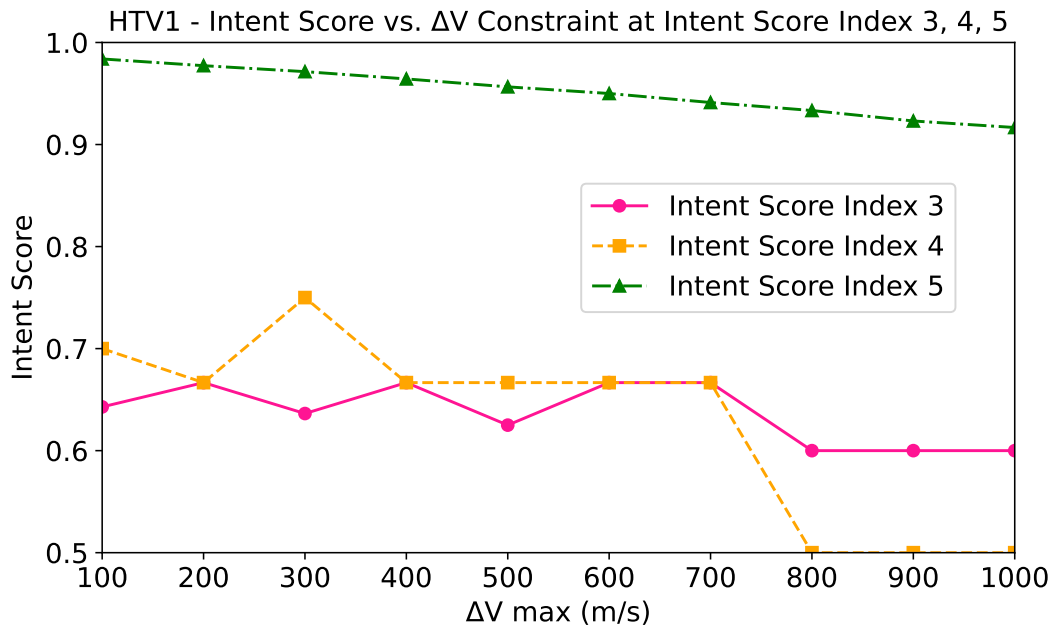


Fig. 5: The figure lists the intent scores at indices 3, 4, and 5 of the HTV-1 resupply to the ISS. See the score indices in Figure 1 and Table 3. The x-axis represents the upper limit of ΔV , and the y-axis represents the intent score. As the figure shows, except for the intent score at index 4, which marginally drops to 0.5 after ΔV at 800 m/s, the other intent scores remain very stable across the range of ΔV maxima.

5.2 USA245 (Blue) and Kosmos 2542/2543 (Red)

Kosmos 2542 and Kosmos 2543 are Russian military satellites of classified purpose. After launch, only Kosmos 2542 was initially detected. Later, a smaller subsatellite, Kosmos 2543, was deployed from Kosmos 2542. Analysis of tracking data shows that from 06/04/2020 to 06/10/2020, Kosmos 2543 was observed to maneuver and approach to around 300 km within USA245 [13]. TLE data can be found at [33, 1] respectively. After 01/15/2020, with no recorded maneuvers and the distance remaining nearly constant at approximately 370 km, the intent score increased from 0.67 to 0.91; see the score indices in Table 4, indicating a potential threat due to likely intentional maneuvers.

Post-Maneuver Analysis (UTC): Intent Score - Red: Russian Kosmos-2543; Blue: USA-245

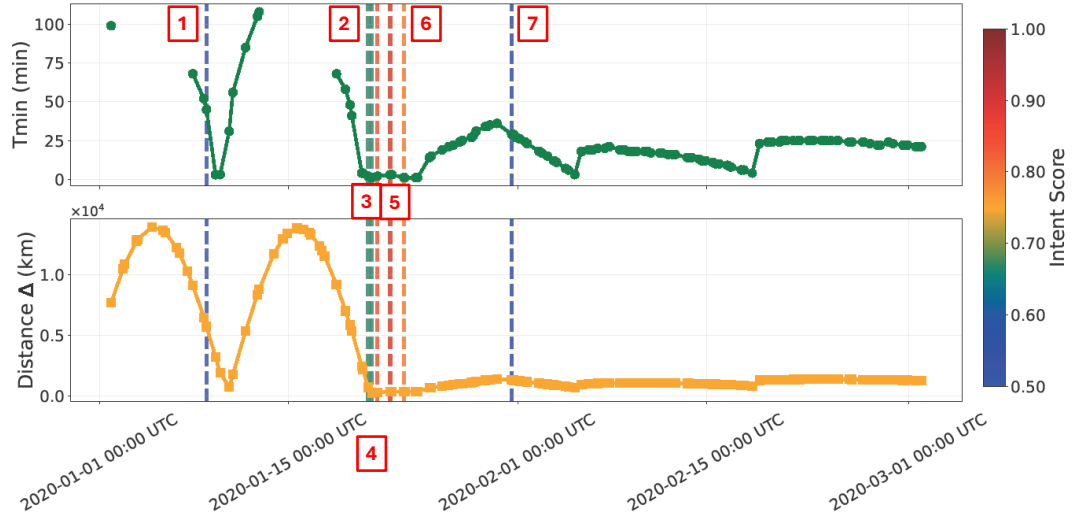


Fig. 6: The top subplot shows the minimum time-to-collision, T_{\min} , and the bottom subplot shows the distance difference between Red and Blue. Vertical dashed lines indicate the intent score, with lower scores shown in blue and higher scores in red; the score is scaled from 0 to 1. In this paper, we define the upper limit of ΔV as 500 m/s, and thus the TOF is subject to this constraint. The figure only shows intent scores greater than 0.5. Notably, after 01/15/2020, despite no documented maneuvers and the distance remaining almost unchanged at approximately 370 km, our intent score increased significantly from the intent score at index 3, which is 0.67, to the intent score at index 5, which is 0.91. This change indicates a possible intentional maneuver. Intent score indices are labeled at the top of the graph. The specific values of intent scores 1–7 are listed in Table 4.

Index	Timestamp (UTC)	Intent Score
1	01/08/2020 10:09 pm	0.51
2	01/20/2020 9:57 pm	0.67
3	01/21/2020 4:26 am	0.67
4	01/21/2020 2:11 pm	0.86
5	01/22/2020 12:57 pm	0.91
6	01/23/2020 1:22 pm	0.80
7	01/31/2020 1:21 pm	0.57

Table 4: USA-245 and Kosmos 2542/2543 intent score with timestamp. The table lists the times of intent score generation as well as the corresponding intent score values. Results are shown with ΔV limited to 500 m/s; only intent scores above 0.5 are included. Scores near 1 indicate a high likelihood of hostile maneuvers, 0.5 indicates no change, and scores near 0 indicate a reduced likelihood. See Figure 6, scores at indices 1–7 are highlighted in red at the top of the graph.

5.3 China SJ-21 (Blue) and China SJ-25 (Red)

The Shijian (SJ) series of satellites, launched by China for dual-use military and civilian applications, includes SJ-25, which conducted a rendezvous maneuver with SJ-21 in late June, approaching the target around 06/30/2025 [12]. TLE data can be found at [46].

Despite the lack of explicit documentation, tracking data indicate that between 06/01/2025 and 06/15/2025, the intent score increased to 0.80, coinciding with a reduction in the measured distance between the two satellites. This demonstrates the robustness of our system, showing that decreases in the distance between two satellites are reliably captured by the intent score.

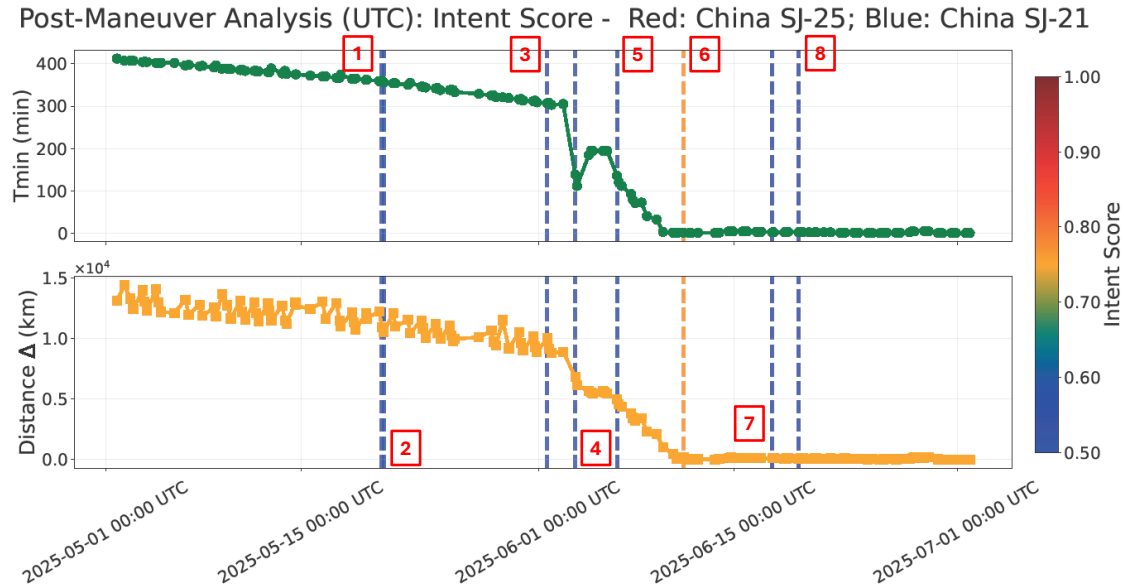


Fig. 7: The top subplot shows the minimum time-to-collision, T_{\min} , and the bottom subplot shows the distance difference between Red and Blue. Vertical dashed lines indicate the intent score, with lower scores shown in blue and higher scores in red; the score is scaled from 0 to 1. In this paper, we define the upper limit of ΔV as 500 m/s, and thus the TOF is subject to this constraint. The figure only shows intent scores greater than 0.5. The highest score is intent score at index 5, which peaks at 0.91. This highest score also aligns with a significant drop in the distance between the two satellites. Intent score indices are labeled at the top of the graph. The specific values of intent scores 1–7 are listed in Table 5.

Index	Timestamp (UTC)	Intent Score
1	05/20/2025 6:39 pm	0.50
2	05/20/2025 10:00 pm	0.50
3	06/01/2025 3:08 pm	0.50
4	06/03/2025 3:20 pm	0.50
5	06/06/2025 3:10 pm	0.59
6	06/11/2025 9:28 am	0.78
7	06/17/2025 6:12 pm	0.57
8	06/19/2025 3:21 pm	0.57

Table 5: China SJ intent score with timestamp. The table lists the times of intent score generation as well as the corresponding intent score values. Results are shown with ΔV limited to 500 m/s; only intent scores above 0.5 are included. Scores near 1 indicate a high likelihood of hostile maneuvers, 0.5 indicates no change, and scores near 0 indicate a reduced likelihood. See Figure 7, scores at indices 1–8 are highlighted in red at the top of the graph

6. CONCLUSION

We present a first-principles, game-theoretic asymmetric pursuit–evasion model with two agents: Red (the pursuer) and Blue (the evader), for early detection and intent scoring of adversarial orbital maneuvers using minimal and incoming TLE data. By combining pursuit–evasion and Stackelberg model with Lambert transfers, our alerting strategy estimates the minimum TOF for potential intercepts under ΔV constraints. Validation on real-world rendezvous events (ISS, USA-245, KOSMOS 2542/2543, China SJ-21/25) demonstrates that our approach can reveal maneuver intent.

In our work, we analyzed system robustness under different ΔV limits. Future work will require a deeper robustness analysis extending to different constraints and variables. Our game requires further numerical analysis to study the behavior predicted by the game-theoretic framework. This formulation introduces a strategic interplay in which Blue must carefully manage its alert budget while attempting to infer whether Red has transitioned to attack mode. Meanwhile, Red must balance between executing deceptive maneuvers before T_A and pursuing an optimal capture strategy after T_A . Based on this setup, we also aim to explore machine learning and reinforcement learning approaches in combination with game theory to better understand and improve Blue’s strategy in the future.

The game structure is modular and enables the study of deception, anticipation, and timing in adversarial scenarios beyond kinetic attacks. Looking ahead, future work should extend the model and test it against a wider range of attack types.

7. REFERENCES

- [1] Elements for s39232. <https://www.planet4589.org/space/elements/39200/S39232> (Accessed 2025-08-18).
- [2] Space domain awareness. Space Doctrine Publication SDP 3-100, United States Space Force, Space Training and Readiness Command (STARCOM), November 2023. OPR: STARCOM Delta 10.
- [3] O. Abdelkhalik and D. Mortari. N-Impulse Orbit Transfer Using Genetic Algorithms. *Journal of Spacecraft and Rockets*, 44(2):456–460, March 2007.
- [4] Annarita Argiro, Maurizio Roseto, Giorgio Isoletta, Roberto Opromolla, Giancarmine Fasano, et al. Catalogue-based screening for in-orbit proximity and threat detection. In *Proceedings of the 75th International Astronautical Congress*, pages 1449–1463, 2024.
- [5] R. R. Bate, D. D. Mueller, and J. E. White. *Fundamentals of Astrodynamics*. Dover Publications, New York, 1971.
- [6] R. H. Battin. *An Introduction to the Mathematics and Methods of Astrodynamics*. AIAA Education Series, 1999.
- [7] R. H. Battin and R. M. Vaughan. An elegant lambert algorithm. *Journal of Guidance, Control, and Dynamics*, 7(6):662–670, 1984.
- [8] S. Baudier, S. Velasco-Forero, F. Jean, D. Brooks, and J. Angulo. Deep matrix profile for maneuver classification in low earth orbit satellite trajectories. In *2024 32nd European Signal Processing Conference (EUSIPCO)*, pages 1781–1785, 2024.
- [9] Center for Strategic and International Studies. Counterspace weapons 101. <https://aerospace.csis.org/aerospace101/counterspace-weapons-101/>, October 28 2019. Last updated June 14, 2022. Accessed August 20, 2025.
- [10] Y. Chen, X. Zhang, W. Liao, G. Wei, and S. Fan. Orbital behavior intention recognition for space non-cooperative targets under multiple constraints. *Aerospace*, 12(520), 2025.
- [11] Y. Chen, X. Zhang, W. Liao, G. Wei, and S. Fan. Orbital Behavior Intention Recognition for Space Non-Cooperative Targets Under Multiple Constraints. *Aerospace*, 12(6):520, June 2025.
- [12] S. Clark. China jumps ahead in the race to achieve a new kind of reuse in space, July 2025. <https://arstechnica.com/space/2025/07/china-jumps-ahead-in-the-race-to-achieve-a-new-kind-of-reuse-in-space/> (Accessed 2025-08-15).
- [13] CNBC. Space force: Russians tracking u.s. spy satellite “unusual and disturbing”, February 2020. <https://www.cnbc.com/2020/02/10/space-force-russians-tracking-us-spy-satellite-unusual-and-disturbing.html> (Accessed 2025-08-15).
- [14] Brandon Collins, Thomas Gherna, Keith Paarporn, Shouhuai Xu, and Philip N Brown. Efficient state estimation of a networked flitpit model. In *64th IEEE Conference on Decision and Control (to appear)*, 2025. <https://arxiv.org/abs/2508.10000>.

[org/pdf/2504.01096](https://www.kth.se/theses/2504.01096).

- [15] M. Dahlman. Methods for co-orbital threat assessment in space. Master's thesis, KTH, 2023.
- [16] P. DiBona, J. Foster, A. Falcone, and M. Czajkowski. Machine learning for RSO maneuver classification and orbital pattern prediction. In S. Ryan, editor, *Advanced Maui Optical and Space Surveillance Technologies Conference*, number 54, page 54, September 2019.
- [17] I. Goumiri, L. Peterson, A. Cocciadiferro, R. Lee, and J. Bernstein. A Common Task Framework for Testing and Evaluation at the Space Domain Awareness Tools, Applications, and Processing Lab. In S. Ryan, editor, *Advanced Maui Optical and Space Surveillance (AMOS) Technologies Conference*, page 93, September 2024.
- [18] M. Guimarães, C. Soares, and C. Manfletti. Data-driven identification of main behavioural classes and characteristics of resident space objects in LEO through unsupervised learning. In S. Ryan, editor, *Advanced Maui Optical and Space Surveillance (AMOS) Technologies Conference*, number 95, page 95, September 2024.
- [19] Colton Hill and Philip N. Brown. Altruism Improves Congestion in Series-Parallel Nonatomic Congestion Games. In *IEEE Conference on Decision and Control (under review)*, apr 2024.
- [20] D. Izzo. Revisiting lambert's problem. *Celestial Mechanics and Dynamical Astronomy*, 121(1):1–15, 2015.
- [21] Japan Aerospace Exploration Agency (JAXA). The htv-1 performed the first height adjustment maneuver. https://iss.jaxa.jp/en/htv/news/htv1_maneuver1.html (Accessed 2025-08-27).
- [22] Japan Aerospace Exploration Agency (JAXA). Htv-1 captured by the international space station, September 2009. https://iss.jaxa.jp/en/htv/news/htv1_capture.html (Accessed 2025-08-15).
- [23] Japan Aerospace Exploration Agency (JAXA). The htv-1 performed the first height adjustment maneuver, September 2009. https://iss.jaxa.jp/en/htv/news/htv1_maneuver1.html (Accessed 2025-08-15).
- [24] K. Johnson, T. G. Roberts, and B. Weedon. Mitigating noncooperative rpos in geosynchronous orbit. *Aether: A Journal of Strategic Airpower & Spacepower*, 1(4):79–94, 2022.
- [25] Katalyst Space Technologies. Space domain awareness (sda). <https://www.katalystspace.com/space-domain-awareness> (Company webpage; Accessed 2025-08-16).
- [26] R. Kato, T. Sakaue, D. Mori, M. Tanaka, T. Sano, K. Taya, M. Ebara, R. Nakazawa, J. Yoshida, and R. Togawa. Validity evaluation of anomaly detection using LSTM autoencoder for maneuver detection. In S. Ryan, editor, *Proceedings of the Advanced Maui Optical and Space Surveillance (AMOS) Technologies Conference*, number 122, page 122, September 2023.
- [27] T. Kelecy and M. Jah. Detection and orbit determination of a satellite executing low thrust maneuvers. *Acta Astronautica*, 66(5):798–809, 2010.
- [28] C. Kiekintveld, T. Islam, and V. Kreinovich. Security Games with Interval Uncertainty. *Proceedings of the 12th International Conference on Autonomous Agents and Multi-agent Systems*, pages 231–238, 2013.
- [29] Y. Ha Kim and D. B. Spencer. Optimal Spacecraft Rendezvous Using Genetic Algorithms. *Journal of Spacecraft and Rockets*, 39(6):859–865, November 2002.
- [30] S. Lemmens and H. Krag. Two-line-elements-based maneuver detection methods for satellites in low earth orbit. *Journal of Guidance Control Dynamics*, 37(3):860–868, May 2014.
- [31] J. Li, Z. Yang, and Y. Luo. Intention inference for space targets using deep convolutional neural network. *Advances in Space Research*, 75(2):2184–2200, 2025.
- [32] L. Liu, B. Li, J. Chen, X. Lei, G. Zhao, and J. Sang. Applying Lambert problem to association of radar-measured orbit tracks of space objects. *Research in Astronomy and Astrophysics*, 21(12):301, December 2021.
- [33] M. McCants. Satellite tracking tle zip files. <https://mmccants.org/tles/index.html> (Accessed 2025-08-18).
- [34] National Aeronautics and Space Administration (NASA). 15 years ago: Japan launches htv-1, its first resupply mission to the space station, September 2024. <https://www.nasa.gov/history/15-years-ago-japan-launches-htv-1-its-first-resupply-mission-to-the-space-station/> (Accessed 2025-08-15).
- [35] T. Nguyen, R. Yang, A. Azaria, S. Kraus, and M. Tambe. Analyzing the Effectiveness of Adversary Modeling in Security Games. *Proceedings of the AAAI Conference on Artificial Intelligence*, 27(1):718–724, jun 2013.
- [36] A. Pastor, G. Escribano, and M. Sanjurjo-Rivo. Satellite maneuver detection and estimation with optical survey observations. *Journal of the Astronautical Sciences*, June 2022.
- [37] F. Quiquet. What are the threats to space systems? <https://www.spacesecurity.info/en/what-are-the-threats-to-space-systems/> (Space & Cybersecurity Info; Accessed 2025-08-21).
- [38] T. Roberts. *Geosynchronous Satellite Maneuver Classification and Orbital Pattern Anomaly Detection via Supervised Machine Learning*. PhD thesis, June 2021.
- [39] Joshua H. Seaton and Philip N. Brown. On the Intrinsic Fragility of the Price of Anarchy. *IEEE Control Systems Letters*, 7:3573–3578, 2023.

- [40] D. Shen, C. Sheaff, G. Chen, J. Lu, M. Guo, E. Blasch, and K. Pham. Game theoretic training enabled deep learning solutions for rapid discovery of satellite behaviors. In Tien Nguyen, editor, *Satellite Systems*, chapter 4. IntechOpen, Rijeka, 2020.
- [41] G. Singh and Sanat K. B. Lambert problem-based maneuver time and delta-v estimation. In *2024 IEEE Space, Aerospace and Defence Conference (SPACE)*, pages 367–369, 2024.
- [42] Vartika Singh, Will Wesley, and Philip N. Brown. Optimal utility design with arbitrary information networks. In *2025 American Control Conference (ACC)*, pages 2895–2900, 2025.
- [43] M. Tambe. *Security and game theory: algorithms, deployed systems, lessons learned*. Cambridge University Press, 2011.
- [44] The Aerospace Corporation. Space domain awareness – sparta. <https://sparta.aerospace.org/countermeasures/CM0077> (The Aerospace Corporation; Accessed 2025-08-20).
- [45] The Associated Press. Hijacked satellites and orbiting space weapons: In the 21st century, space is the new battlefield. <https://apnews.com/article/space-weapons-trump-satellites-russia-0fdd31a1e3d350a54823e8a3d228fc17> (AP News; Accessed 2025-08-20).
- [46] United States Space Force and 18th Space Defense Squadron. Space-track.org. <https://www.space-track.org/auth/login> (Official USSF portal for SSA data; account required; Accessed 2025-08-16).
- [47] T. Valentinova, P. De Marchi, D. Oltrogge, J. Cornelius, D. A. Vallado, F. Caronte, and N. Casciola. Watch out GEO satellites, here’s a new ML-method for manoeuvre detection and intent classification. In *4th International Conference on Space Situational Awareness (ICSSA)*, Daytona Beach, FL, USA, May 2024.
- [48] D. A. Vallado. *Fundamentals of Astrodynamics and Applications*. Microcosm Press, 4th edition, 2013.
- [49] H. Von Stackelberg. *Market structure and equilibrium*. Springer Science & Business Media, 2010.
- [50] I. E. Weintraub, M. Pachter, and E. Garcia. An Introduction to Pursuit-evasion Differential Games. In *2020 American Control Conference (ACC)*, pages 1049–1066. IEEE, jul 2020.
- [51] J. West, W. Wark, and A. Shull. The importance of satellites to life on earth. <https://www.cigionline.org/multimedia/the-importance-of-satellites-to-life-on-earth/> (Centre for International Governance Innovation (CIGI); Accessed 2025-08-20).
- [52] S. Wishnek. A minimal observation method for high-thrust initial maneuver determination. *The Journal of the Astronautical Sciences*, 72, June 2025.
- [53] D. Witman, T. Olson, B. Williams, D. Kesler, and B. Marchand. Action-Free Inverse Reinforcement Learning for Evaluating Satellite Similarity and Anomaly Detection. In S. Ryan, editor, *Advanced Maui Optical and Space Surveillance (AMOS) Technologies Conference*, page 18, September 2024.